4d Electronic structure analysis of ruthenium in the perovskite oxides by Ru K- and L-edge XAS

Jong-Young Kim,[a] Sung-Ho Hwang,[a] Seung-Joo Kim [b] and Gérard Demazeau,[b] Jin-Ho Choy,[a*] Hiromichi Shimada[c]

[a]National Nanohybrid Materials Laboratory, School of Chemistry and Molecular Engineering, Seoul National University, Seoul 151-742, Korea, [b]Institut de Chimie de la Matière de Condenseé de Bordeaux(ICMCB), Avenue de Dr. Schweitzer, 33608 Pessac Cedex, France,[c]National Institute of Materials and Chemical Research, 1-1 Higashi, Tsukuba, Ibaraki 305, Japan.
Email:jhchoy@plaza.snu.ac.kr

The 4*d* electronic structure of ruthenium in the perovskite oxides, $La_2MRu^{IV}O_6$ (M = Zn, Mg, and Li) and $Ba_2YRu^{V}O_6$, has been investigated by the Ru K-and L-edge XANES and EXAFS analyses. Such X-ray absorption spectroscopic results clarify that the Ru^{IV} (d^4) and Ru^{V} (d^3) ions are stabilized in nearly regular O_h site. Comparing the Ru L-edge XANES spectra of perovskites containing isovalent ruthenium, it has been found that the t_{2g} state is mainly influenced by A site cation, whereas the e_g is mainly affected by neighboring B site cation. The experimental EXAFS spectra in the range of R ≤ ~ 4.5 Å are well reproduced by ab-initio calculation based on crystallographic data, which supports the long-range structure presented by Rietveld refinement.

Keywords : Electronic Structure, Ruthenium, XAS

1.Introduction

The L-edge XANES spectroscopy is a very powerful tool to understand electronic structure of transition metal compounds since it exhibits prominent features due to the transition from the $2P_{3/2}$ level to unoccupied *nd* states which is primarily responsible for the variation of local symmetry and chemical bonding. As shown in previous L_{III}-edge XANES study on 5*d* transition metals (Choy et al.,1994 & 1995), the relative position and area of the main absorption edge can be well interpreted by the one-electron approximation and crystal field theory. Especially, our interest is focussed on perovskite-type oxides having the general formula $A_2BB'O_6$, in which the B-O bond has to compete with the B'-O and A-O bonds by sharing the same oxygen 2*p* orbital with pathways 180° and 90°, respectively. (Goodenough, 1971) In this perovskite system, the electronic structure of B' element can be finely tuned by controlling the size and electronegativity of the A and B cations. Here, we report the results of the Ru L-edge X-ray absorption spectra for some ruthenates and attempt to understand the relationship between the electronic structure of ruthenium and the covalency of the (Ru-O) bond. The matrices of La_2MRuO_6 (M = Zn, Mg, and Li) and Ba_2YRuO_6 were chosen to stabilize definitely the Ru^{IV} and Ru^{V} ions, and the local chemical environment around ruthenium was controlled by the competing A and B site cations.

2.Experimental

1.1. *Sample preparation*

Polycrystalline samples of La_2MRuO_6 (M = Li, Mg, and Zn), and Ba_2YRuO_6 were prepared by firing stoichiometric amounts of reactants $La(CH_3CO_2)_3$, ZnO, Y_2O_3, $(MgCO_3)_4{\cdot}Mg(OH)_2{\cdot}5H_2O$, RuO_2, and excess $Li(OH){\cdot}H_2O$ to compensate for the sublimation of Li_2O during high temperature synthesis. The reaction mixtures were heated at the following temperatures for several days in air, with intermittant grindings : La_2MgRuO_6 at 1150°C, La_2ZnRuO_6 at 1050°C, La_2LiRuO_6 at 800°C, and Ba_2YRuO_6 at 1300°C. For La_2LiRuO_6, an oxygen gas pressure of 1 kbar (100 MPa) was applied at 800°C over 48 hr using a compressed gas apparatus.

2.2. *X-ray absorption spectroscopy*

The X-ray absorption measurements on the Ru K-edge and L-edge were carried out with synchrotron radiation at the beam lines 10B and 11B, respectively, of the Photon Factory (KEK-PF) in Tsukuba. For the Ru K-edge measurements, the samples were ground to fine powders in a mortar with Boron nitride as a diluent and pelleted to obtain an optimum absorption jump ($\Delta\mu_t \approx 1$). For the Ru L-edge measurements, the pelleted samples were used and the data were recorded in the total electron yield mode in UHV chamber (ca.10^{-9} torr). The data analysis was performed according to the previously published procedures (Choy et al., 1994 & 1995). Ab-initio curved wave multiple scattering EXAFS spectra were computed by FEFF6 (Rehr et al., 1992) using the atomic coordinates according to the Rietveld refinement results of La_2MRuO_6 (M=Li, Mg, and Zn) and the reported crystallographic data of Ba_2YRuO_6. The amplitude reduction factors for all the paths were constrained to the best fitted values of single shell fitting. The Debye-Waller factors for the first shells were set to the best fitted values of single shell fitting and those for further shells were varied to appropriate values ($3.5\text{-}6.0\times10^{-3}$/Å^2) for reproducing the experimental spectra well. The multiple scattering paths contributing a mean-path amplitude greater than 5% of that of the first shell maximum, as estimated by FEFF's curved wave calculation, were included in the final calculation.

3.Result and Discussion

1.2. *Ru L_{III}-edge XANES spectra*

As shown in Fig. 1, the Ru L_{III}-edge XANES spectra exhibit two peaks which are ascribed to the electric dipole allowed transitions from Ru 2*p* level to 4*d* ones (t_{2g} and e_g) split by the crystal field in octahedral symmetry. The peak positions (Et_{2g} and Ee_g) and energy splitting ($\Delta E = Ee_g - Et_{2g}$) are mainly influenced by the oxidation state of ruthenium ion. The higher the oxidation state of the ruthenium ion is, the greater the covalency of the Ru-O bond becomes, and as a consequence, the transition energy and crystal field splitting becomes larger. The energy splitting, ΔE, is not exactly equal to the crystal field parameter, 10*Dq*, because it is determined in the $2p^5 4d^{n+1}$ final states instead of the $4d^n$ ground states.(de Groot et al., 1990) However, if the same electronic configuration and similar local symmetry are retained, the final state effect might remain the same in magnitude and, therefore, can be cancelled out. Therefore, a careful comparison of the XANES spectra can provide a way of estimating the covalency of the Ru-O bond.

The metal-oxygen bonding character is susceptible not only to the oxidation state but also to the change of neighboring cations and anions. Since the Ru and M cations are ordered in octahedral sites of A_2MRuO_6, the $\sigma_{Ru\text{-}O}$ and $\pi_{Ru\text{-}O}$ bonds should compete with $\sigma_{M\text{-}O}$ and $\sigma_{A\text{-}O}$ ones, respectively.(Goodenough, 1971) Therefore, a weakened interaction between M and O would reinforce the $\sigma_{Ru\text{-}O}$ bond, resulting in the destabilization of the anti-bonding e_g level on the basis of the molecular orbital concept of a single cluster (RuO_6). In the same way, the weaker A-O interaction makes the $\pi_{Ru\text{-}O}$ bond stronger, and hence the antibonding t_{2g} level becomes higher. The crystal field splitting

between the e_g and t_{2g} levels in the d-state can be affected by both these factors.

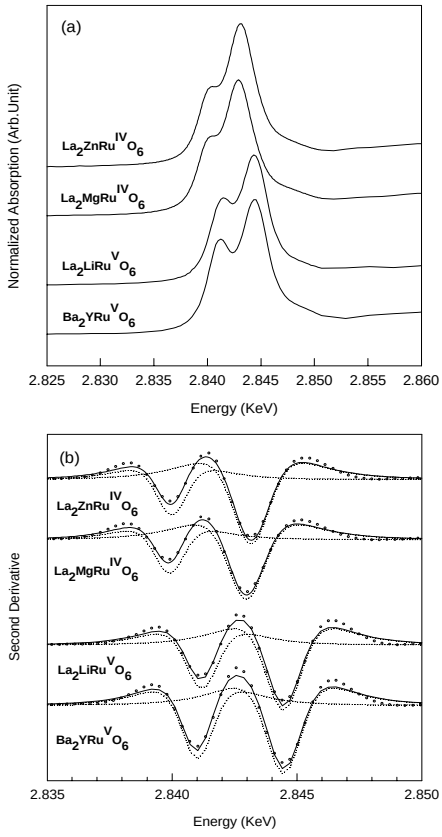

Figure 1. (a) Normalized Ru L_{III}-edge spectra and (b) their second derivatives for La_2MRuO_6 (M = Zn, Mg and Li) and Ba_2YRuO_6.

Since the La_2MgRuO_6 and La_2ZnRuO_6 compounds have the same A site cation (La) and isovalent ruthenium ion (Ru^{IV}), only a factor influencing the Ru-O bond covalency is the B site cations, Mg and Zn. We can expect a greater destabilization of the e_g level for La_2MgRuO_6 than for La_2ZnRuO_6 as a result of weaker competition of $\sigma_{Ru\text{-}O}$ bond with $\sigma_{Mg\text{-}O}$ one. In the present spectra, Ee_g for Mg compound is 0.20 eV higher than that for Zn one, whereas Et_{2g} is only 0.08 eV higher. Therefore, the larger splitting for La_2MgRuO_6 (ΔE = 3.18 eV) than that for La_2ZnRuO_6 (ΔE=3.07 eV) indicates that the $\sigma_{Ru\text{-}O}$ bond covalency is enhanced by the relatively ionic $\sigma_{Mg\text{-}O}$ one.

In case of La_2LiRuO_6 and Ba_2YRuO_6 containing Ru^V ion, a stronger destabilization of the antibonding e_g level is expected for the former when only the B site elements (Li and Y) are considered due to the fact that the lithium has higher Lewis acidity. However, the Ee_g values seem to be not so significantly influenced as shown in Table 1 (2844.45 and 2841.46 eV for La_2LiRuO_6 and Ba_2YRuO_6, respectively), which is thought to be due to the fact that the La_2LiRuO_6 compound has a monoclinic lattice where Li-O-Ru bond angle is severely distorted to *ca*.155° unlike a cubic Ba_2YRuO_6. Owing to the nonlinear Li-O-Ru chain, the pathway for effective competition between $\sigma_{Li\text{-}O}$ bond and $\sigma_{Ru\text{-}O}$ one is disturbed, which precludes the destabilization of antibonding e_g level. On the other hand, unlike the σ-bond, which is sensitive to the linearity of M-O-Ru chain, the competition involving the π-bond is less sensitive to the bond angle.(Goodenough, 1971) The fact that the t_{2g} level is lower for La_2LiRuO_6 (2841.00 eV) than for Ba_2YRuO_6 (2841.18 eV) can be rationalized on the basis of the competition of $\sigma_{A\text{-}O}$ bond with $\pi_{Ru\text{-}O}$ bond. The stronger $\sigma_{La\text{-}O}$ bond, caused by the higher Lewis acidity of the lanthanum ion compared to the barium ion, weakens $\pi_{Ru\text{-}O}$ bond, resulting in a lower Et_{2g}. Consequently, ΔE of La_2LiRuO_6 (3.46 eV) is larger than that of Ba_2YRuO_6 (3.27 eV).

The total integrated peak areas (At_{2g} and Ae_g) in XANES spectra provides further valuable information on the number of available orbitals for the transition. The $2p \rightarrow t_{2g}$ transition for Ru^{IV} shows a much smaller peak area than that for Ru^V, whereas the $2p \rightarrow e_g$ transition shows almost constant peak area irrespective of the oxidation state. This implies that Ru^{IV} is different from Ru^V in the hole density of only in t_{2g} states, which means that the electronic configurations are ($t_{2g}^4e_g^0$) for Ru^{IV} and ($t_{2g}^3e_g^0$) for Ru^V. The ratios (At_{2g}/Ae_g) of *ca*. 0.31 for Ru^{IV} and 0.53 for Ru^V are rather smaller than the values expected from the statistical *d* counts of the t_{2g} and e_g states, 0.5 and 0.75 (number of holes for t_{2g} / number of holes for e_g). It was reported that this effect is due to several factors such as measurement conditions, spin exchange effect (George et al., 1990), and different thermal effects (de Groot et al., 1990) on the t_{2g} and e_g states. Nevertheless, it is worthy to note here that the ratio $(At_{2g}/Ae_g)_{Ru}{}^{V}$ / $(At_{2g}/Ae_g)_{Ru}{}^{IV}$, 1.7, is nearly coincident with the ratio (1.5) of numbers of holes for each t_{2g} level with the configurations ($t_{2g}^3e_g^0$) and ($t_{2g}^4e_g^0$) indicating that this ratio cancels out the factors affecting the peak area except for the covalency and oxidation state effects.

Table 1. Energy values for t_{2g} and e_g electronic states (Et_{2g} and Ee_g) and peak area (*A*) of the second derivatives of Ru L_{III}-edge XANES spectra.

	Position (*E*/eV)			Area (*A*/eV)	
Compounds	$E_{t_{2g}}$	E_{e_g}	ΔE	$A_{t_{2g}}$	A_{e_g}
La_2MgRuO_6	2839.97	2843.16	3.19	16.9	55.0
La_2ZnRuO_6	2839.89	2842.96	3.07	16.0	51.0
Ba_2YRuO_6	2841.18	2844.45	3.27	23.6	47.2
La_2LiRuO_6	2841.00	2844.46	3.46	27.9	49.3

3.2. *Ru K-edge EXAFS spectra*

The Fourier transforms (FTs) of the Ru K-edge EXAFS spectra in R space are shown in Fig. 2a. The fitting results for Fourier-filtered shell in the range of ~0.5 Å ≤ R ≤ ~2 Å, are also represented in Fig. 2a. The resulting $k^3\chi(k)$ filtered EXAFS oscillations (open circles) and their best fits (solid lines) in the range of ~2 $Å^{-1}$ ≤ k ≤ ~14 $Å^{-1}$ are plotted in Fig. 2b. The structural parameters obtained from EXAFS analysis are shown in Table 2. The first peak in R space, attributed to the Ru-O bonding pair, is quite intense and highly isotropic, which suggests nearly regular O_h symmetry of the RuO_6 octahedron. It is also noticeable that FTs spectra in higher R range, 2.5 Å ≤ R ≤ 4.5 Å, show quite different shapes between cubic Ba_2YRuO_6 phase and monoclinic La_2MRuO_6 one (M = Zn, Mg, and Li). In general, as the Ru-O-M chain loses its linearity by distortion, the intensity in this range would be significantly reduced. In addition, the single scattering (Ru-La) contribution is strongly depressed by disordered distribution of A site cations due to monoclinic distortion. From this fact, the weak intensity in the spectra for La_2MRuO_6 (M = Zn, Mg, and Li) can be explained by monoclinic distortion. Debye-Waller factors (σ^2) have the values in the range of 2.5-3.3×10^{-3} ($Å^2$). The slightly larger values of σ^2 for the Ru^{IV}-O bonding pair are interpreted as a result of strong thermal vibration due to their large bond distance compared to that of Ru^V-O. According to the structural data obtained by Rietveld

refinement, EXAFS spectra were computed up to ~4.5 Å including multiple scattering terms over third order (four-legged paths). The experimental and calculated FT spectra with multiple scattering paths are compared in Fig. 3. The most important contributions are those from three single scatterings (SS), one collinear double scattering (CDS), and two collinear triple scatterings (CTS). The SS paths correspond to oxygen atoms, A site cations, and another B site (M) one. In particular, in the range 3~4.5 Å, CTS1 (Ru-O1-Ru-O2-Ru), CTS2 (Ru-O1-M-O1-Ru), and CDS (Ru-O-M-Ru) paths become more important as a result of the well-known focussing effect. (Stern et al.,1981; Lee et al., 1975) In this region, various oscillations interfere with each other destructively or constructively and, furthermore, the number of paths is enormously increased up to ~200 for $R \leq 6$ Å by monoclinic distortion. Therefore, it is impossible to determine structural parameters (R, σ^2, S_o^2, ΔE_o) and to obtain physically meaningful information. However, the experimental data are well reproduced by ab-initio calculation based on crystallographic data, which supports the long-range structure represented by Rietveld refinement.

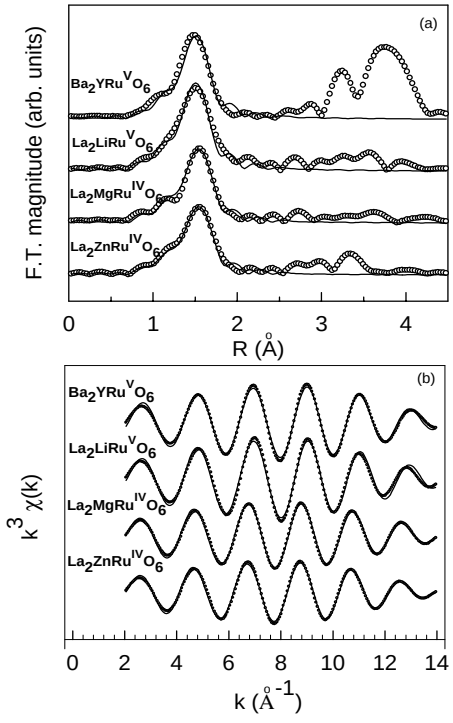

Figure 2. (a) Fourier transform (open circle) and best fit (solid line) of Ru K-edge EXAFS spectra, and (b) Fourier-Filtered EXAFS spectra (symbol: experimental; solid line: fitting result) in the first coordination sphere of the Ru-O bonding pair.

Table 2. Bond distances and Debye-Waller factors for Ru-O bond obtained from EXAFS and XRD Rietveld refinements.

Compounds	Debye-Waller factor ($\times 10^{-3}$ Å^2)	Average (Ru-O) Bond distance (Å)	
		EXAFS	Rietveld refinement
La_2MgRuO_6	2.8_9	1.99_1	1.99(3)
La_2ZnRuO_6	3.3_1	1.99_6	1.99(3)
La_2LiRuO_6	2.4_6	1.94_8	1.93(2)
Ba_2YRuO_6	2.6_3	1.95_3	1.954

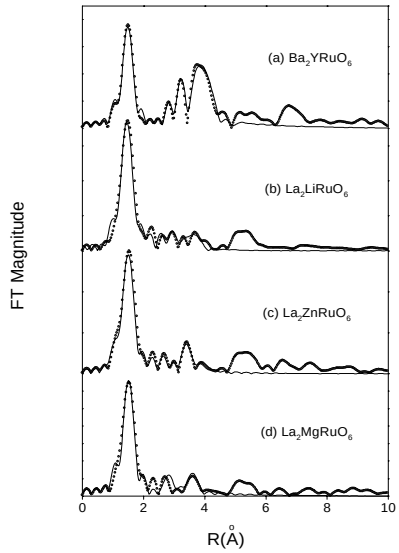

Figure 3. Fourier transformed experimental data (open circles) and ab-initio computations (solid line) including multiple scattering up to $R \leq$ ~4.5 Å for (a) Ba_2YRuO_6, (b) La_2LiRuO_6, (c) La_2ZnRuO_6, and (d) La_2MgRuO_6.

This work is financially supported by the Ministry of Education through Korea Reseach Foundation (1997-011-D0019) and BK 21 program and by the Ministry of Science and Technology (NRL project).

References

Choy, J. H., Kim, D.K., Demazeau, G.& Jung, D.Y. (1994) *J. Phys. Chem.* **98**, 6258.
Choy, J.H., Kim, D.K., Hwang, S. H., Demazeau, G.& Jung, D.Y. (1995) *J. Am. Chem. Soc.* **117**, 8557.
Rehr, J.J., Zabinsky, S.I., Albers, R.C.(1992) *Phys. Rev. Lett.* **69**, 3397.
Goodenough , J.B. (1971) *Prog. Solid State Chem.* **5**, 145.
Battle, P.D.& Jones, C.W. (1989) *J. Solid State Chem.* **78**, 108.
de Groot, F.M., Fuggle, J.C., Thole, B.T.& Sawatzky, G.A. (1990) *Phys. Rev. B*, **42**, 5459.
George, G.N., Cleland, W.E., Enemark, J.H., Smith, B.E., Kipke, C.A., Robert, S.A.& Cramer, S.P. (1990) *J. Am. Chem. Soc.* **112**, 2541.
Stern, E.A., Bunker, B.& Heald, S.M. (1981) *Phys. Rev. B*, **28**, 3520.
Lee, P.A.& Pendry, J.B. (1975) *Phys. Rev. B*, **11**, 2795.